Claudin-2 expression induces cation-selective channels in tight junctions of epithelial cells

Salah Amasheh[1], Noga Meiri[1], Alfred H. Gitter[1], Torsten Schöneberg[3], Joachim Mankertz[2], Jörg D. Schulzke[2] and Michael Fromm[1,*]

[1]Department of Clinical Physiology, [2]Department of Gastroenterology, Infectiology and Rheumatology, and [3]Department of Pharmacology, Benjamin Franklin Medical School, Freie Universität Berlin, Hindenburgdamm 30, 12200 Berlin, Germany

*Author for correspondence (e-mail: michael.fromm@medizin.fu-berlin.de)

Accepted 11 September 2002
Journal of Cell Science 115, 4969-4976 © 2002 The Company of Biologists Ltd
doi:10.1242/jcs.00165

Summary

Tight junctions seal the paracellular pathway of epithelia but, in leaky tissues, also exhibit specific permeability. In order to characterize the contribution of claudin-2 to barrier and permeability properties of the tight junction in detail, we studied two strains of Madin-Darby canine kidney cells (MDCK-C7 and MDCK-C11) with different tight junctional permeabilities.

Monolayers of C7 cells exhibited a high transepithelial resistance (>1 kΩ cm^2), compared with C11 cells (<100 Ω cm^2). Genuine expression of claudin-1 and claudin-2, but not of occludin or claudin-3, was reciprocal to transepithelial resistance. However, confocal microscopy revealed a marked subjunctional localization of claudin-1 in C11 cells, indicating that claudin-1 is not functionally related to the low tight junctional resistance of C11 cells.

Strain MDCK-C7, which endogenously does not express junctional claudin-2, was transfected with claudin-2 cDNA. In transfected cells, but not in vector controls, the protein was detected in colocalization with junctional occludin by means of immunohistochemical analyses. Overexpression of claudin-2 in the originally tight epithelium with claudin-2 cDNA resulted in a 5.6-fold higher paracellular conductivity and relative ion permeabilities of Na^+≡1, K^+=1.02, $NMDG^+$=0.79, $choline^+$=0.71, Cl^-=0.12, Br^-=0.10 (vector control, 1:1.04:0.95:0.94:0.85:0.83). By contrast, fluxes of (radioactively labeled) mannitol and lactulose and (fluorescence labeled) 4 kDa dextran were not changed. Hence, with regular Ringer's, Na^+ conductivity was 0.2 mS cm^{-2} in vector controls and 1.7 mS cm^{-2} in claudin-2-transfected cells, while Cl^- conductivity was 0.2 mS cm^{-2} in both cells. Thus, presence of junctional claudin-2 causes the formation of cation-selective channels sufficient to transform a 'tight' tight junction into a leaky one.

Key words: Zonula occludens, Claudins, Occludin, Transepithelial resistance, Impedance analysis

Introduction

Occludin was the first transmembrane protein discovered in the tight junction (TJ) (Furuse et al., 1993), suggesting a physiological role in maintaining the TJ structure and function, including gate and fence properties (Balda et al., 1996). However, its functional role has been questioned by recent knockout studies, showing that occludin-deficient epithelial cells still possess TJ strands (Saitou et al., 1998). Moreover, the knockout mouse model did not display a perturbation of epithelial barrier function, although a complex pathophysiological phenotype was observed with growth retardation, chronic inflammation and hyperplasia of the gastric epithelium, and calcification in the brain (Saitou et al., 2000).

The claudin family shows an organ- and tissue-specific expression of individual members. Deficiency or aberrant expression of distinct claudins has been reported to be associated with severe pathophysiological consequences (for a review, see Anderson, 2001; Tsukita et al., 2001). Claudin-1-deficient mice die within one day of birth because of loss of epidermal barrier function (Furuse et al., 2002). Further defects were autosomal recessive deafness in the case of claudin-14 (Wilcox et al., 2001), hypomagnesaemia, which is associated with mutations of claudin-16 (Simon et al., 1999), and the fact that CNS myelin and sertoli cell TJ strands are absent in Osp/claudin-11 null mice (Gow et al., 1999). Details concerning functional properties of single claudins have been described for claudin 2, 4 and 15. Furuse et al. demonstrated that expression of claudin-2 is correlated with a decrease of transepithelial resistance (Furuse et al., 2001). However, the first direct demonstration of the ability of a claudin to influence paracellular ion selectivity was contributed by Van Itallie et al. for claudin-4 (Van Itallie et al., 2001). In addition, Colegio et al. showed that the first extracellular domain of claudin-4 is responsible for this property and that expression of wild-type claudin-15 leads to an increase in transepithelial resistance (Colegio et al., 2002).

There are two twin strains of Madin-Darby canine kidney (MDCK) cells with markedly different transepithelial resistance, MDCK I and II (Richardson et al., 1981) and MDCK-C7 and -C11 (Gekle et al., 1994). Recently, Furuse et al. reported that those with a high resistance (MDCK I) lack claudin-2, and that expression of claudin-2 lowers the transepithelial resistance (Furuse et al., 2001). This is a most important finding, although a decrease in transepithelial resistance does not prove that paracellular, rather than transcellular, pathways were affected.

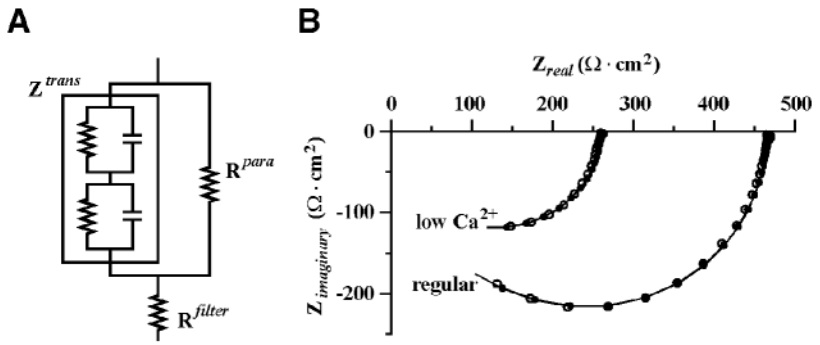

Fig. 1. Transepithelial impedance analysis. (A) Electrical equivalent circuit of the epithelium. See Materials and Methods for explanation. (B) Typical impedance data (open circles) of an C7-cld-2 monolayer (transfected with claudin-2 cDNA) in regular Ringer's solution and in low Ca^{2+} Ringer's. The Nyquist plot shows the real and the imaginary parts of the transepithelial impedance as a function of frequency. Dots on a solid line depict the least-squares fit of the data to the electrical model.

Beyond the approach of Tsukita et al., we employed confocal laser scanning microscopy, impedance analysis, biionic/dilution potential measurements, and tracer flux experiments. The results demonstrate that claudin-2 is responsible for the formation of a paracellular, cation-selective pore.

Materials and Methods

Cells and solutions

Experiments were performed on monolayers of MDCK-C7 and -C11 cell strains (Gekle et al., 1994). Cells were grown in 25 cm^2 culture flasks containing MEM-EARLE (Biochrom, Berlin, Germany). Medium was supplemented with 10% (v/v) fetal bovine serum, 100 U/ml penicillin and 100 mg/ml streptomycin (Biochrom, Berlin, Germany) at 37°C in a humidified 5% CO_2 atmosphere.

For electrophysiological measurements and molecular analyses, epithelial cell monolayers were grown on porous polycarbonate culture plate inserts (effective area 0.6 cm^2, Millicell^{TM}-HA, Millipore, Bedford, MA). On day 7, resistance and impedance analyses were performed. Inserts were mounted in Ussing chambers, and water-jacketed gas lifts were filled with 10 ml circulating fluid on each side. The standard bathing ringer solution contained: 113.6 mM NaCl, 2.4 mM Na_2HPO_4, 0.6 mM NaH_2PO_4, 21 mM $NaHCO_3$, 5.4 mM KCl, 1.2 mM $CaCl_2$, 1.2 mM $MgCl_2$, 10 mM D(+)-glucose. According to the respective experimental approach, low (20 nM), and high (12.6 mM) Ca^{2+} concentrations (impedance analysis) were employed, or NaCl was partially substituted during flux and dilution potential experiments. All solutions were gassed with 95% O_2 and 5% CO_2, to ensure a pH value of 7.4 at 37°C.

Electrophysiology

Short-circuit current (I_{SC}, μmol h^{-1} cm^{-2}) and transepithelial resistance, referring to tissue area (R^{epi}, Ω cm^2), were measured in Ussing chambers specially designed for insertion of Millicell filters (Kreusel et al., 1991). Resistance of bathing solution and filter support (R^{filter}) was measured prior to each single experiment and subtracted. Impedance analysis was performed to characterize the paracellular component of the transepithelial resistance of MDCK monolayers as described previously (Gitter et al., 1997a; Gitter et al., 1997b). Briefly, a programmable frequency response analyzer in combination with an electrochemical interface (models 1250 and 1286, Solartron Schlumberger, Farnborough, UK) was employed for application of sinusoidal currents, logarithmically spaced in frequencies from 1 kHz to 65 kHz. The electrical equivalent circuit of the epithelium comprises an ohmic paracellular pathway (R^{para}) and a transcellular pathway with capacitive components (representing cell membranes) resulting in a complex impedance (Z^{trans}).

The circuit model is shown in Fig. 1A. Impedance (Z^{epi}) was plotted in Nyquist diagrams (Fig. 1B). In each experiment with C7 monolayers, the paracellular resistance, R^{para}, was changed by lowering the extracellular Ca^{2+} concentration. In the case of C11 monolayers, the reduced Ca^{2+} concentration led to a complete breakdown of the epithelial barrier and, therefore, the extracellular Ca^{2+} concentration was increased resulting in a higher R^{para}. In each case it was assumed, however, that the perturbation (ctrl→ΔCa) affected R^{para}, but not Z^{trans}.

$$Z^{epi}[ctrl] = \frac{1}{(1/Z^{trans}) + (1/R^{para}[ctrl])}$$

$$Z^{epi}[\Delta Ca] = \frac{1}{(1/Z^{trans}) + (1/R^{para}[\Delta Ca])}$$

The two sets of data, differing in R^{para}, allowed subtraction of Z^{trans}. Hence, the fit of impedance data with the equations of the electrical model allowed evaluation of R^{para}.

Flux and dilution/biionic potential measurements

Measurement of unidirectional tracer flux from the apical to the basolateral side was performed under short-circuit conditions with 25 kBq/ml of [^{3}H]-mannitol or [^{3}H]-lactulose (Biotrend, Cologne, Germany). The medium also contained non-labeled tracer molecules (10 mM mannitol or 10 mM lactulose, respectively). Four 15-minute flux periods were analyzed (Schultz and Zalusky, 1964). Upon initiation and completion, a 100 μl sample was taken from the donor (apical) side, and 900 μl Ringer's and 4 ml of Ultima Gold high flash-point liquid scintillation cocktail (Packard Bioscience, Groningen, The Netherlands) were added. Samples (1 ml) of the receiving (basolateral) side, replaced with fresh Ringer's, were mixed with 4 ml of the liquid scintillation cocktail. All 5 ml samples were subsequently analyzed with a Tri-Carb 2100TR Liquid Scintillation counter (Packard, Meriden, CT). In 4 kDa FITC-dextran flux analyses the high molecular weight fluorescent dye was dissolved in Ringer's at a concentration of 25 mg/ml and dialyzed against the same buffer. This solution was employed in the basolateral compartment. After 5 hours incubation the amount of FITC-dextran in the apical compartment was measured with a fluorometer at 520 nm (Spectramax Gemini, Molecular devices, Sunnyvale, CA).

Dilution and biionic potentials were measured with modified Ringer's solution on the mucosal or serosal side, and the data from both conditions were pooled. In the modified Ringer's, 70 mM NaCl were replaced by KCl, NMDGCl, NaBr or choline chloride. Relative ion permeabilities were calculated by means of the Goldman-Hodgkin-Katz equation and partial ion conductivities were determined using the respective ion concentrations of normal Ringer's.

Immunofluorescence studies

Immunofluorescence analysis and photography were performed as

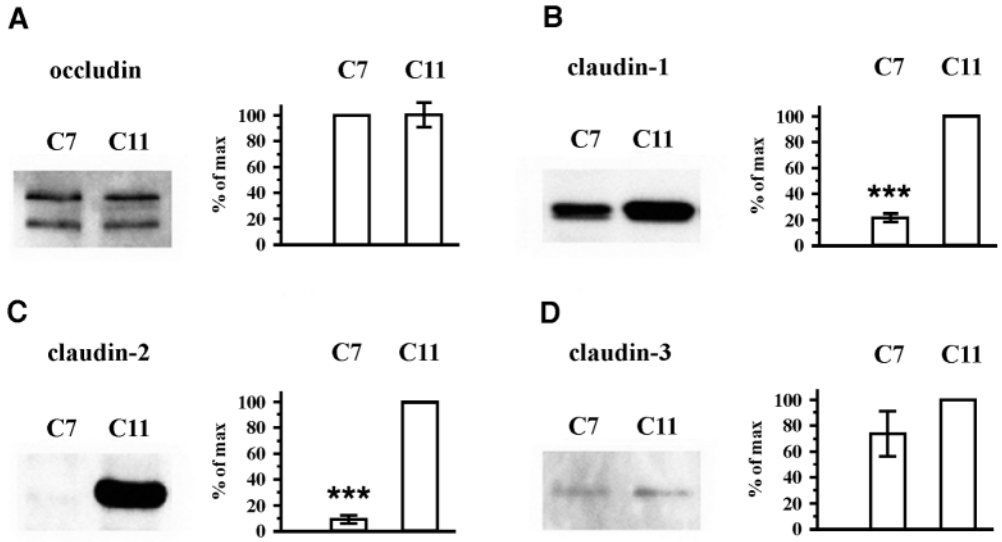

Fig. 2. Expression of tight junction proteins in MDCK-C7 and C11. Western blots and densitometry. 2.5 µg of samples were loaded on SDS gel, electrophoresed, blotted and genuine expression of occludin, claudin-1, -2 and -3 was detected using polyclonal antibodies. Densitometric analysis of western blots was performed using quantification software (see Materials and Methods), Expression of occludin (A) and claudin-3 (D) did not differ significantly, whereas claudin-1 (B) and -2 (C) were lower in C7 (n=4-6).

described (Weiske et al., 2001). Cells were grown on coverslips (18×18 mm, Menzel, Braunschweig, Germany). For immunological studies, cells were rinsed with PBS, fixed with methanol, and permeabilized with PBS containing 0.5% Triton X-100. Concentrations of primary antibody were 20 µg/ml (Ms anti-occludin, Rb anti-claudin-1, -2, -3; Zymed Laboratories, San Francisco, CA). Secondary ABs Alexa Fluor 488 goat anti-mouse and Alexa Fluor 594 goat anti-rabbit (both used in concentrations of 2 µg/ml) were purchased from Molecular Probes (MoBiTec, Göttingen, Germany). Fluorescence images were obtained with a confocal microscope (Zeiss LSM510) using excitation wavelengths of 543 nm and 488 nm. Details of the microscopy setup are available upon request.

PCR cloning of mouse claudin-2 from mouse colon RNA

Total RNA was obtained from mouse distal colon using RNAzol B reagent (WAK Chemie, Bad Soden, Germany). First strand cDNA was synthesized by reverse transcriptase reaction (M-MLV, Gibco BRL, Bethesda, MD) employing oligo(dT) primer. Sense (5′-GTCTGCCA-TGGCCTCCCTTG-3′) and antisense (5′-CAGCTCTGGCCCCTG-GTTCT-3′) primers were synthesized according to the mouse claudin-2 sequence (Furuse et al., 1998) and used for PCR. The resulting 720 bp PCR product encompassing the complete claudin-2 cDNA was cloned into pGEMT-Easy (Promega, Madison, WI). The correctness of the cDNA was verified by sequencing and then subcloned into the eukaryotic expression vector pcDNA3.1 (Invitrogen, Carlsbad, CA) further referred to as p[cld-2]. MDCK-C7 cells were stably transfected with p[cld-2] by employing the Lipofectamine plus method (Gibco BRL, Bethesda, MD). G418-resistant cell clones were screened for claudin-2 expression by western blot (see below). C7 and C11 cells transfected with an empty vector (p[vec]) served as controls.

Western blotting

Cells were washed in ice cold PBS, scraped from the permeable supports in Tris-buffer containing 20 mM Tris, 5 mM $MgCl_2$, 1 mM EDTA, 0.3 mM EGTA, and protease inhibitors (Complete, Boehringer, Mannheim, Germany). Protein was obtained by freeze-thaw cycles and subsequent passage through a 26 G ½ needle. The membrane fraction was obtained by two centrifugation steps: first, samples were centrifuged for 5 minutes at 200 ***g*** (4°C); then, supernatant was centrifuged for 30 minutes at 43,000 ***g*** (4°C). The pellet was resuspended in Tris-buffer and protein content was determined using BCA Protein assay reagent (Pierce, Rockford, IL) quantified with a plate reader (Tecan, Austria). After measurement of total membrane protein, 2.5 µg of the samples were mixed with SDS buffer (Laemmli), loaded on a 12.5% SDS polyacrylamide gel and electrophoresed. Proteins were detected by immunoblotting employing antibodies raised against human occludin and claudin-1, -2 and -3. All primary antibodies were provided from Zymed Laboratories (San Francisco, CA). Specific signals were quantified with luminescence imaging (LAS-1000, Fujifilm, Japan) and quantification software (AIDA, Raytest, Germany).

Statistical analysis

Data are expressed as means±standard error of the mean. Statistical analysis was performed using Student's t-test and the Bonferroni correction for multiple comparisons. $P<0.05$ was considered significant.

Results

TJ protein expression is different in MDCK-C7 and -C11 cells

To analyze the contribution of occludin and individual members of the claudin family to barrier function we used kidney epithelium cell lines MDCK clones C7 and C11 which show a characteristic difference in transepithelial resistance. C7 exhibited a high resistance (1056±74 Ω cm^2, n=17), whereas transepithelial resistance of C11 was approximately 20-fold lower (52±1 Ω cm^2, n=17).

To biochemically characterize the potential mechanism of these obvious differences, expression levels of TJ proteins were quantified by immunoblotting. As shown in Fig. 2, expression of occludin (Fig. 2A) was identical in both cell lines. Occludin migrated as two main bands with apparent molecular weights ranging from 55 to 67 kDa probably due to post-translational modification or occurrence of splice variants. The most obvious difference was observed for claudin-2, which was markedly expressed in C11 but only marginally detected in C7 cells (8.9±1.9% of expression in C11, n=6). In C7 cells, lower expression was also detected for claudin-1 (21.3±3.1% of expression in C11, n=5), whereas claudin-3 did not differ significantly between the two strains C7 and C11 (73.6±18%

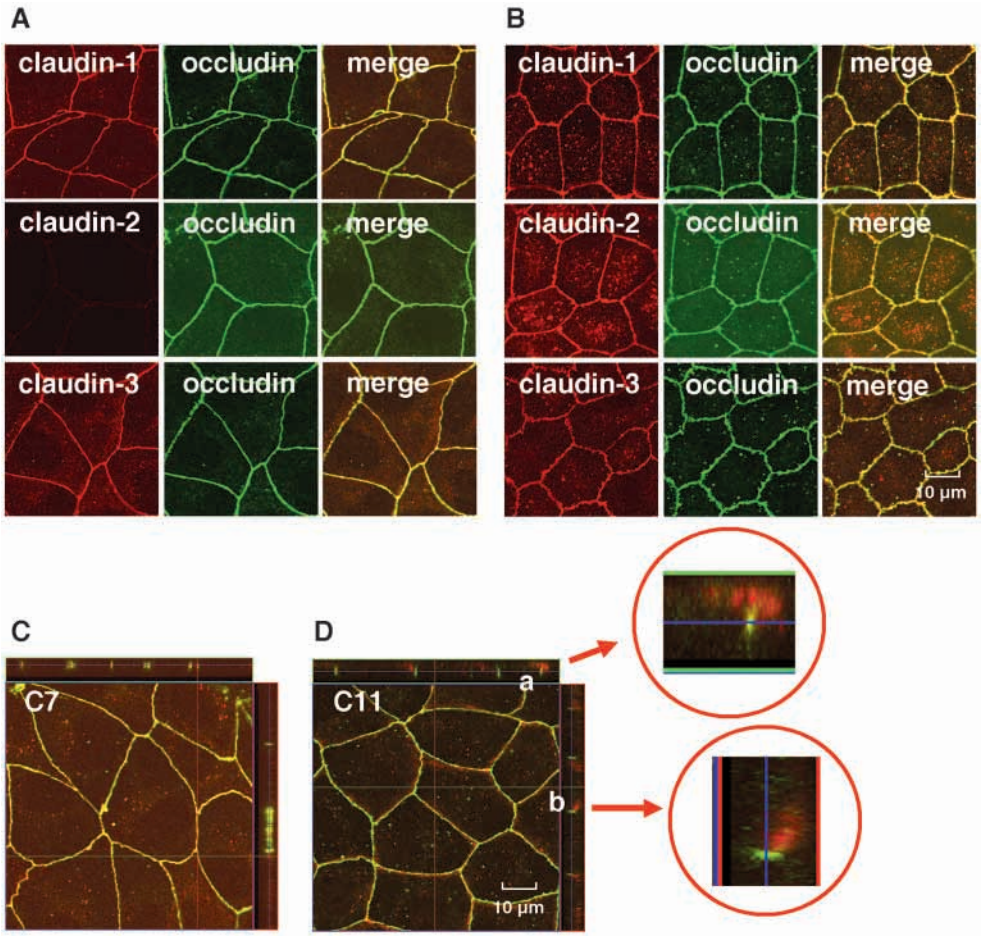

Fig. 3. Analyses of the subcellular distribution of TJ proteins. Immunofluorescence studies of claudins-1, -2 and -3 (red) and occludin (green) in MDCK-C7 (A), and -C11 (B) cells were performed using the confocal microscope technique (see Materials and Methods). Colocalization (yellow) was detected for all claudins, except for claudin-2 in MDCK-C7. Z-scans (C,D) as shown on the right or above the top views were performed in 200 nm steps over a range of 10 µm. The Z-scans of claudin-1 in C7 (C) and C11 (D) revealed that a marked expression of claudin-1 is detectable in subjunctional membrane areas in C11 (circles).

of expression in C11, n=4). All claudins were detected as a 22 kDa band (Fig. 2).

Next, immunofluorescence studies were performed to characterize the subcellular distribution of occludin and claudins in MDCK cell lines C7 and C11. Confocal microscope analysis demonstrated a genuine colocalization of claudin 1 and 3 with occludin in both C7 and C11, whereas in accordance with western blot analyses claudin-2 expression was detectable only in C11 (Fig. 3A,B). Z-scans of confocal images revealed that the high expression of claudin-1 in the leaky cell strain C11 is not limited to the strand region but is concentrated in subjunctional areas (Fig. 3C,D).

Transfected MDCK-C7 cells stably express claudin-2

For functional analyses of claudin-2, which is endogenously expressed at high levels in the leaky strain MDCK-C11, the protein was overexpressed in MDCK-C7, the high resistance strain with weak genuine claudin-2 expression.

Transfection resulted in a detectable expression of claudin-2 as shown by western blot studies, whereas expression of claudin-1 did not change (Fig. 4A). As a result, a dramatic decrease of epithelial resistance was observed after transfection (R^{epi}, 27.6±0.7% compared with 100% control R^{epi}; n=3, Fig. 4B) while no change of paracellular 4K FITC-dextran flux was detectable (n=6, Fig. 4C). The subcellular distribution of claudin-2 in the transfected clones of C7 cells was analyzed by immunological studies in combination with confocal microscopy techniques. While no expression of claudin-2 was detected in C7 cells transfected with vector alone (C7-vec; Fig. 4D), claudin-2 was found to be colocalized with the TJ protein occludin in C7 transfected with claudin-2 cDNA (C7-cld-2; Fig. 4E,F).

Paracellular cation permeability

To functionally characterize the clones, impedance analyses, flux measurements and dilution/biionic potential measurements were performed. In leaky epithelia, such as MDCK clone C11, the transepithelial resistance R^{epi} mainly depends on the resistance of the paracellular pathway, R^{para}, and evaluation of R^{epi} (by measuring the response to DC electric current) is a good estimate of the junctional barrier to paracellular ion movement. It is important to note, however, that in tight epithelia, such as clone C7, R^{para} cannot be estimated from R^{epi} because R^{epi} of tight epithelia is mainly determined by the bouquet of channels and carriers within the cell membranes. We therefore determined R^{para} from impedance analysis (Fig. 5). In monolayers of C7 cells transfected with claudin-2 (C7-cld-2), R^{para} was 5.6-fold lower than in clone C7-vec without claudin-2 (485±14 Ω cm^2, n=4 vs. 2734±119 Ω cm^2, n=4, P<0.001). However, compared with C11, cells transfected with vector alone (C11-

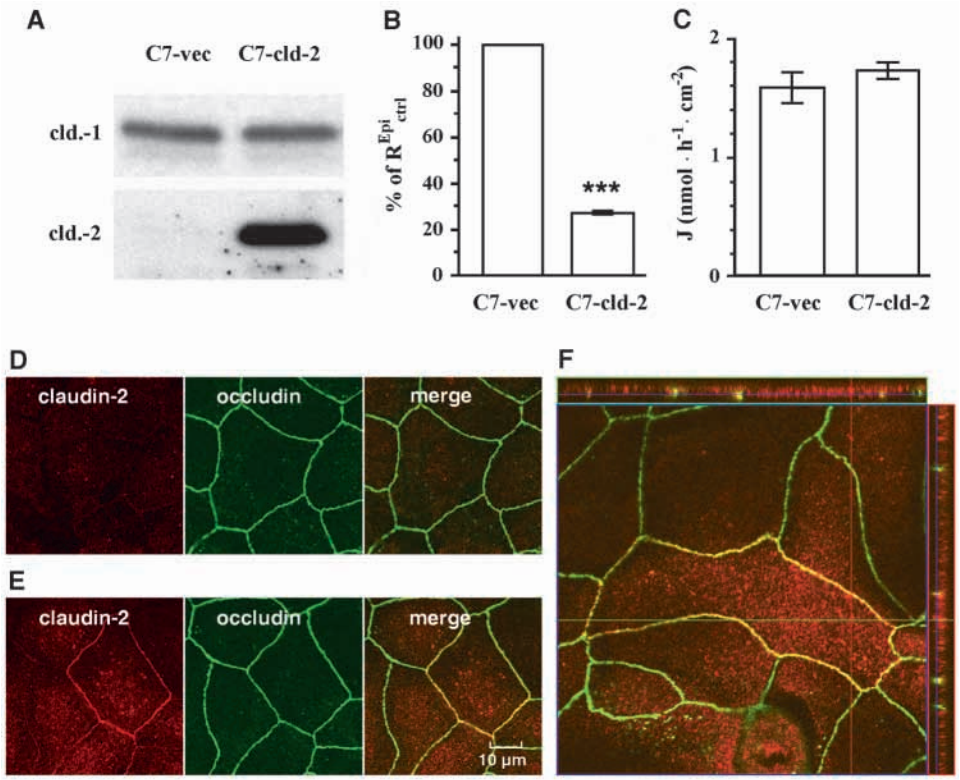

Fig. 4. (A) Transfection of C7 with claudin-2 cDNA. Western blots detecting claudin-1 and claudin-2 in MDCK clones stably transfected with claudin-2 cDNA (C7-cld-2), compared with control (transfected with vector alone, C7-vec). (B) Decrease of R^{epi} by introducing claudin-2 into MDCK-C7 cells. (C) Permeability of 4K FITC dextran in C7-vec and C7-cld-2. (D,E) Comparison of claudin-2 expression in the different clones using a confocal microscope. Detection of claudin-2 (red) and occludin (green) in C7-vec (D) and in C7-cld-2 (E). Transfectants did not show detectable changes in claudin-1 and -3 (not shown). F) Z-scans of C7-cld-2 detecting occludin (green) and claudin-2 (red). Scans as shown on the right or above the top views were performed in 200 nm steps over a range of 10 µm. A tight junctional colocalization of claudin-2 with occludin is observed.

vec: 68±2 Ω cm^2, n=4, P<0.001), R^{para} was 7.1-fold higher in C7-cld-2.

Charge selectivity was assessed with measurement of NaCl dilution potentials. The ratio of Na^+ to Cl^- permeability (P_{Na}/P_{Cl}) was 1.19±0.05 (n=6) in C7-vec and increased to 8.7±0.4 (n=6, P<0.001) in C7-cld-2. Hence, expression of claudin-2 created a cation-selective passive pathway. The permeability ratio of Br^- to Cl^- was 0.985±0.004 (n=6) in C7-vec and decreased to 0.869±0.022 (n=6, P<0.01) in C7-cld-2. In comparison, clone C11-vec showed a ratio of 0.685±0.009 (n=6, P<0.01). Measurements of biionic potentials revealed that Na^+ and K^+ permeabilities were not significantly different in all three clones. The permeability ratio of Na^+ to choline$^+$ (104.2 Da), was 33% higher in C7-cld-2, and 3.6 times higher in C11, than in C7-vec. The permeability ratio of Na^+ to $NMDG^+$ was 20.5% higher in C7-cld-2, and 2.7 times higher in C11-vec. These experiments demonstrated the size discrimination of claudin-2 channels. From measurements of dilution and biionic potentials relative paracellular permeabilities were calculated according to the Goldman-Hodgkin-Katz equation (Fig. 6A). Thus, transfection of C7 cells resulted in a change of relative ion permeabilities from 1 Na^+ : 1.043±0.02 K^+ : 0.95±0.006 $NMDG^+$: 0.941±0.021 choline$^+$: 0.846±0.034 Cl^- : 0.834±0.034 Br^- to 1 Na^+ : 1.022±0.006 K^+ : 0.79±0.016 $NMDG^+$: 0.705±0.013 choline$^+$: 0.116±0.006 Cl^- : 0.101±0.006 Br^-; relative permeabilities of C11 were 1 Na^+ : 1.033±0.002 K^+ : 0.351±0.008 $NMDG^+$: 0.277±0.03 choline$^+$: 0.023±0.003 Cl^- : 0.015±0.002 Br^- (n=6, Fig. 6A).

Flux measurements employing [^{3}H]-mannitol (184 Da) or [^{3}H]-lactulose (342.5 Da), revealed that transfection of C7 with claudin-2 cDNA does not lead to an increased paracellular permeability for molecules of ≥184 Da, although permeability of both molecules was higher in the C11 clone (Fig. 6B). Partial ion conductivities were calculated from relative paracellular permeabilities of Na^+, K^+, $NMDG^+$, Cl^- and Br^- (Fig. 6C). Clone C7-cld2 showed a selective increase of Na^+ and K^+ conductance compared with C7 control (Na^+: 1.739±0.064 mS cm^{-2} vs. 0.208±0.014 mS cm^{-2}; K^+: 0.069±0.003 mS cm^{-2} vs. 0.008±0.001 mS cm^{-2}), whereas Cl^- conductance was not significantly changed (0.178±0.011 mS cm^{-2} vs. 0.155±0.012 mS cm^{-2}).

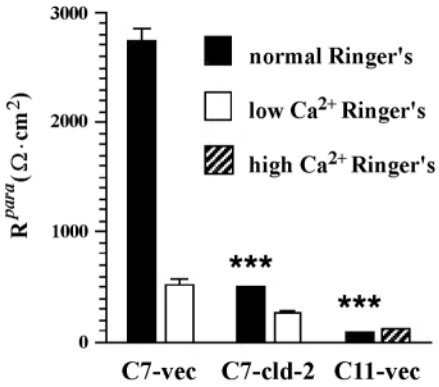

Fig. 5. Paracellular resistance (R^{para}) of MDCK monolayers as derived from transepithelial impedance analysis. In monolayers of C7-cld-2 (transfected with claudin-2 cDNA), R^{para} was lower (P<0.001) than in clone C7-vec (transfected with vector only), although higher (P<0.001) than in MDCK clone C11-vec. With low Ca^{2+} Ringer solution, R^{para} decreased in the C7 clones. In C11-vec exposed to high Ca^{2+} Ringer's, R^{para} increased.

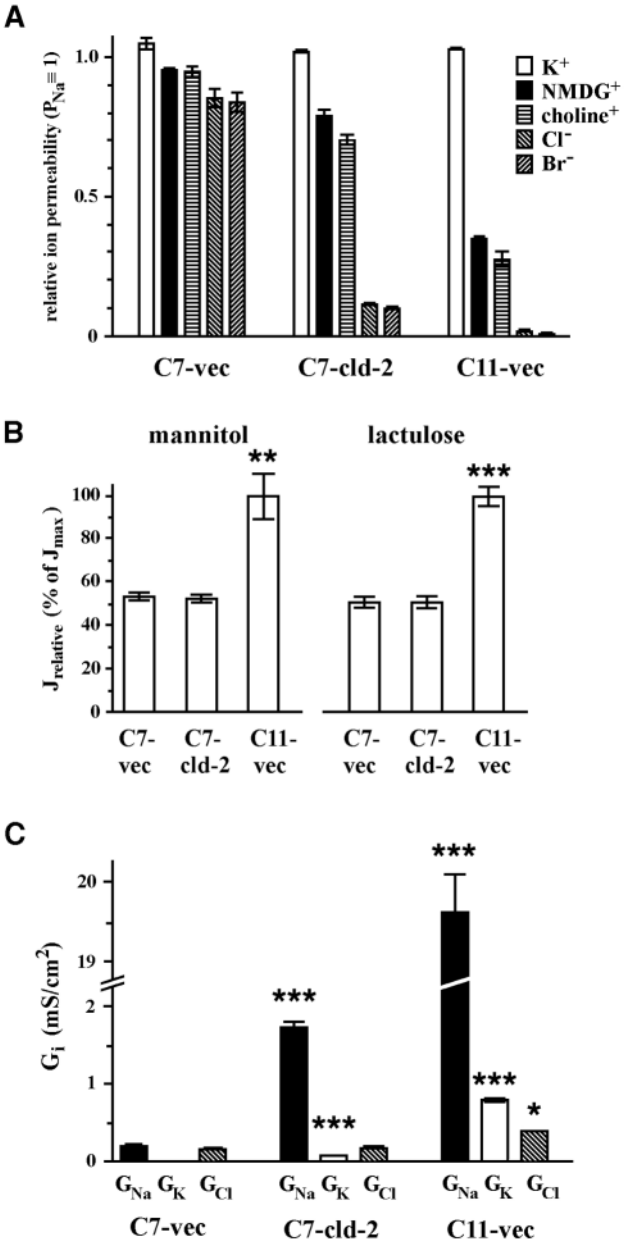

Fig. 6. (A) Relative permeabilities with reference to Na^+ (defined as 1) for K^+, $NMDG^+$, $choline^+$, Cl^- and Br^- in C7-vec, C7-cld2, and C11-vec, as derived from measurement of biionic (Na^+/K^+, $Na^+/NMDG^+$, $Na^+/choline^+$) and dilution potentials (Na^+/Cl^-, Na^+/Br^-, n=6). Lower values compared with C7-vec were detected for $NMDG^+$, $choline^+$, Cl^- and Br^- in both clones C7-cld-2 and C11-vec (P<0.001). (B) Permeabilities for mannitol and lactulose were calculated from ^{3}H-mannitol and ^{3}H-lactulose fluxes and were not significantly different in monolayers of MDCK clone C7 without or with transfection with claudin-2 cDNA (n=4 and 6, respectively), although they were lower than in clone C11-vec (n=4 and 6, respectively, P<0.05). (C) Partial ion conductivities calculated for Na^+, K^+ and Cl^- in C7-vec, C7-cld-2 and C11-vec (n=6). Because Na^+ and K^+ were almost equally permeable but Na^+ is 26-fold higher concentrated than K^+, the contribution of Na^+ to overall conductivity is about 25-fold of that of K^+.

Discussion

Cation permeability depends on expression of claudin-2

The presence of claudin-2 has been reported in the epithelia of many organs, including liver and kidney (Furuse et al., 1998), as well as gut, liver and pancreas (Rahner et al., 2001). The first details concerning the functional role of claudin-2 have been reported recently. Expression of claudin-2 decreases the overall transepithelial resistance in MDCK cells (Furuse et al., 2001). This was a landmark finding showing that claudin-2 is associated with a conductance increase, but cellular/paracellular localization of that conductance as well as its ion specificity is unresolved so far. Large paracellular markers (4 kDa and 40 kDa FITC-dextran) do not pass (Furuse et al., 2001). Therefore we characterized the claudin-2-induced conductivity regarding localization, ion selectivity and size requirements.

Impedance analysis

The simultaneous fit of an electrical model to the data recorded under the different conditions yielded values for R^{para} that (1) hardly varied with the start parameters of the fit algorithm, and (2) were reproducible in repeated measurements. The parameters of transcellular pathways were indeterminate and, therefore, not interpreted. Because of their reproducibility, the values of R^{para} may be considered a measure of the junctional barrier function. In the case of the low-resistance C11 clone, a similar value of R^{para} had been found previously with a different method [conductance scanning (Gitter et al., 1997b)]. This correspondence defies a systematic error and supports the validity of the present method.

Single recordings of the transepithelial impedance under one experimental condition cannot resolve R^{para} (Kottra and Frömter, 1984), but additional information is gained by a controlled perturbation in only one parameter of the system. Since changes of the extracellular Ca^{2+} concentration are an established tool for the modulation of TJs [Ca^{2+} switch (Contreras et al., 1992)], we measured the frequency dependence of transepithelial impedance in the same epithelium at two different Ca^{2+} concentrations, assuming this affected only R^{para}. As expected, R^{para} decreased in the C7 clones incubated with low Ca^{2+} Ringer solution. In C11 cells exposed to high Ca^{2+} Ringer, R^{para} increased.

Claudin-2 expression leads to the presence of paracellular cation channels

Paracellular resistance, a measure of the tight junctional barrier, decreased after transfection with claudin-2, but the transepithelial flux of labeled mannitol, lactulose, and 4 kDa dextran did not change. Hence, claudin-2 induces paracellular ion channels not permeable to uncharged molecules >182 Da. In addition, biionic and dilution potential measurements revealed a selectivity with the permeability sequence $K^+ \approx Na^+ > NMDG^+ > choline^+ >> Cl^- = Br^-$. This sequence is indicative of a pronounced cation selectivity.

The colocalization of claudin-2 and occludin in the area of the tight junctions provides evidence against an indirect intracellular effect of claudin-2 modulating the tight junctions, but there is still the possibility that claudin-2 has regulatory function only and the conductive site is located somewhere else, either in the transcellular route (trans-

membranal channels or conductive carriers) or in the paracellular path (other tight junction proteins). Regarding the first alternative, we have shown for the first time for any claudin-induced conductance change that it is localized directly in the paracellular pathway. With this result a regulatory effect on trans-membranal channels or carriers is excluded (Fig. 1). Thus, the only possibility of an indirect effect of claudin-2 would be that it regulates the conductivity of other claudins (or of occludin or JAM). Although we cannot strictly exclude this possibility, from the molecular structure we have no indication that claudin-2 simply by its presence alters the structure of other claudins to a cation conductive state.

In our experiments, expression of claudin-2 after transfection resembled 'genuine' expression levels (as detected in C11 cells), indicating that changes can be attributed to physiological claudin-2 properties, and not necessarily to a changed expression ratio of other claudins. This is supported by the finding that after transfection other claudins did not show detectable changes of expression levels.

The concentration of claudin-1 in the subjunctional region of C11 cells indicates that elevated expression levels of a single claudin may not necessarily result in exclusive localization of that claudin within the tight junction.

The functional changes induced by expression of claudin-2 are opposite to the changes associated with overexpression of claudin-4. Van Itallie et al. found a decrease of paracellular sodium permeability after claudin-4 overexpression in MDCK cells (Van Itallie et al., 2001).

The hypothesis that single claudins create ion-selective paracellular channels has been supported by Colegio et al., demonstrating that reversing the charge of a single amino acid in the first extracellular loop of claudin-4 dramatically changes epithelial permeability (Colegio et al., 2002).

Claudin-1 expression

In MDCK cells claudin-1 has been shown to increase resistance (Inai et al., 1999; McCarthy et al., 2000). The most striking evidence showing responsibility of claudin-1 for barrier function has been presented in a claudin-1-knockout study: claudin-1 molecules expressed in the epidermis are indispensable for creating and maintaining the epidermal barrier (Furuse et al., 2002). Whereas these studies unequivocally show a resistance increase and barrier formation of claudin-1, at first sight the results of our study indicate a resistance decreasing role of claudin-1.

Closer inspection using confocal microscopy solved the puzzle: in contrast to claudin-2, claudin-1 was predominantly found below the tight junction. This finding is supported by Gregory et al., who demonstrated that claudin-1 expression in epithelial cells is not localized exclusively in tight junctions, but appears along the entire interfaces of adjacent epithelial cells as well as along the basal plasma membrane (Gregory et al., 2001). Hence, claudin-1 is not necessarily colocalized with occludin in the TJ, and the higher conductivity of the C11 clone can be explained by claudin-2 expression alone.

In the present experimental design we selectively changed the expression of claudin-2 in the C7 cells, while the amount of claudin-1 was not changed. The functional changes described here must therefore be attributed to the effect of claudin-2.

Claudin-3 expression

Claudin-3 was found in equal amounts in both strains C7 and C11, and was always colocalized with occludin in the tight junction. Therefore, claudin-3 appears to be a constitutive transmembranal TJ protein. Data from claudin-3 transfection experiments have been published previously (Furuse et al., 2001). The authors reported no change of functional properties of the TJ excluding a functional role in the difference between the high and low resistance strains. Nevertheless, the importance of this protein was highlighted when a specific binding of Clostridium perfringens enterotoxin to claudin-3 and -4 was reported. In contrast, no correlation with claudin-1 and -2 could be found (Sonoda et al., 1999; Fujita et al., 2000).

Occludin expression

Occludin has been demonstrated to be an important component of the tight junction, as elevated expression caused strand numbers to increase, followed by a rise of transepithelial resistance and a decrease of mannitol flux (McCarthy et al., 1996). In addition, truncation of the C-terminus leads to an increase of paracellular flux (Balda et al., 1996; Chen et al., 1997). Furthermore, a loss of fence function was observed, leading to a free diffusion of lipids from the apical to the basolateral membrane domain (Balda et al., 1996). Occludin colocalization with members of the claudin family has been reported (Tsukita and Furuse, 1998). An important aspect of tight junctional regulation emerged from studies comparing occludin with claudin-4 (Balda et al., 2000). In this study, multiple occludin domains were demonstrated to be involved in regulation of paracellular permeability. By contrast, potential dispensability of the presence of occludin in TJs was demonstrated in knockout experiments: although complex morphological changes emerged from this approach, no effect on transepithelial resistance was observed (Saitou et al., 2000). These findings suggested either that occludin is not primarily responsible for determination of the paracellular barrier or that possible splice variants were not afflicted in the knockout experiments. As, in our approach, the expression did not differ in low- and high-resistance MDCK cells under all experimental conditions, occludin turned out to be a suitable reference molecule for TJ location.

Conclusion

The decrease in transepithelial resistance induced by expression of claudin-2 is caused by a distinct paracellular ion permeability. The ion permeability sequence is $Na^+=K^+ > NMDG^+ > choline^+ >> Cl^-=Br^-$. Fluxes of conventional paracellular markers are not increased. Claudin-2 localizes at the tight junction. Thus, we suggest that junctional claudin-2 forms or induces cation-selective channels in tight junctions of epithelial cells.

MDCK strains were a gift from Hans Oberleithner (Department of Physiology, University of Münster, Germany). The superb assistance

of Anja Fromm, Ursula Lempart, Ingrid Lichtenstein, and Sieglinde Lüderitz is gratefully acknowledged.

References

Anderson, J. M. (2001). Molecular structure of tight junctions and their role in epithelial transport. *News Physiol. Sci.* **16**, 126-130.

Balda, M. S., Whitney, J. A., Flores, C., Gonzalez, S., Cereijido, M. and Matter, K. (1996). Functional dissociation of paracellular permeability and transepithelial electrical resistance and disruption of the apical-basolateral intramembrane diffusion barrier by expression of a mutant tight junction membrane protein. *J. Cell Biol.* **134**, 1031-1049.

Balda, M. S., Flores-Maldonado, C., Cereijido, M. and Matter, K. (2000). Multiple domains of occludin are involved in the regulation of paracellular permeability. *J. Cell Biochem.* **78**, 85-96.

Chen, Y., Merzdorf, C., Paul, D. L. and Goodenough, D. A. (1997). COOH terminus of occludin is required for tight junction barrier function in early Xenopus embryos. *J. Cell Biol.* **138**, 891-899.

Colegio, O. R., van Itallie, C. M., McCrea, H. J., Rahner, C. and Anderson, J. M. (2002). Claudins create charge-selective channels in the paracellular pathway between epithelial cells. *Am. J. Physiol. Cell Physiol.* **283**, C142-C147

Contreras, R. G., Miller, J. H., Zamora, M., Gonzalez-Mariscal, L. and Cereijido, M. (1992). Interaction of calcium with plasma membrane of epithelial (MDCK) cells during junction formation. *Am. J. Physiol.* **263**, C313-C318.

Fujita, K., Katahira, J., Horiguchi, Y., Sonoda, N., Furuse, M. and Tsukita, S. (2000). Clostridium perfringens enterotoxin binds to the second extracellular loop of claudin-3, a tight junction integral membrane protein. *FEBS Lett.* **476**, 258-261.

Furuse, M., Hirase, T., Itoh, M., Nagafuchi, A., Yonemura, S., Tsukita, S. and Tsukita, S. (1993). Occludin: a novel integral membrane protein localizing at tight junctions. *J. Cell Biol.* **123**, 1777-1788.

Furuse, M., Fujita, K., Hiiragi, T., Fujimoto, K. and Tsukita, S. (1998). Claudin-1 and claudin-2: novel integral membrane proteins localizing at tight junctions with no sequence similarity to occludin. *J. Cell Biol.* **141**, 1539-1550.

Furuse, M., Furuse, K., Sasaki, H. and Tsukita, S. (2001). Conversion of Zonulae occludentes from tight to leaky strand type by introducing claudin-2 into Madin-Darby canine kidney I cells. *J. Cell Biol.* **153**, 263-272.

Furuse, M., Hata, M., Furuse, K., Yoshida, Y., Haratake, A., Sugitani, Y., Noda, T., Kubo, A. and Tsukita, S. (2002). Claudin-based tight junctions are crucial for the mammalian epidermal barrier: a lesson from claudin-1-deficient mice. *J. Cell Biol.* **156**, 1099-1111.

Gekle, M., Wünsch, S., Oberleithner, H. and Silbernagl, S. (1994). Characterization of two MDCK-cell subtypes as a model system to study principal cell and intercalated cell properties. *Pflügers Arch.* **428**, 157-162.

Gitter, A. H., Schulzke, J. D., Sorgenfrei, D. and Fromm, M. (1997a). Ussing chamber for high-frequency transmural impedance analysis of epithelial tissues. *J. Biochem. Biophys. Methods* **35**, 81-88.

Gitter, A. H., Bertog, M., Schulzke, J. D. and Fromm, M. (1997b). Measurement of paracellular epithelial conductivity by conductance scanning. *Pflügers. Arch.* **434**, 830-840.

Gow, A., Southwood, C. M., Li, J. S., Pariali, M., Riordan, G. P., Brodie, S. E., Danias, J., Bronstein, J. M., Kachar, B. and Lazzarini, R. A. (1999). CNS myelin and sertoli cell tight junction strands are absent in Osp/claudin-11 null mice. *Cell* **99**, 649-659.

Gregory, M., Dufresne, J., Hermo, L. and Cyr, D. G. (2001). Claudin-1 is not restricted to tight junctions in the rat epididymis. *Endocrinology* **142**, 854-863.

Inai, T., Kobayashi, J. and Shibata, Y. (1999). Claudin-1 contributes to the epithelial barrier function in MDCK cells. *Eur. J. Cell Biol.* **78**, 849-855.

Kottra, G. and Frömter, E. (1984). Rapid determination of intraepithelial resistance barriers by alternating current spectroscopy. I. Experimental procedures. *Pflügers Arch.* **402**, 409-420.

Kreusel, K. M., Fromm, M., Schulzke, J. D. and Hegel, U. (1991). Cl^- secretion in epithelial monolayers of mucus forming human colon cells (HT-29/B6). *Am. J. Physiol.* **261**, C574-C582.

McCarthy, K. M., Skare, I. B., Stankewich, M. C., Furuse, M., Tsukita, S., Rogers, R. A., Lynch, R. D. and Schneeberger, E. E. (1996). Occludin is a functional component of the tight junction. *J. Cell. Sci.* **109**, 2287-2298.

McCarthy, K. M., Francis, S. A., McCormack, J. M., Lai, J., Rogers, R. A., Skare, I. B., Lynch, R. D. and Schneeberger, E. E. (2000). Inducible expression of claudin-1-myc but not occludin-VSV-G results in aberrant tight junction strand formation in MDCK cells. *J. Cell Sci.* **113**, 3387-3398.

Rahner, C., Mitic, L. L. and Anderson, J. M. (2001). Heterogeneity in expression and subcellular localization of claudins 2, 3, 4, and 5 in the rat liver, pancreas, and gut. *Gastroenterology* **120**, 411-422.

Richardson, J. C., Scalera, V. and Simmons, N. L. (1981). Identification of two strains of MDCK cells which resemble separate nephron tubule segments. *Biochim. Biophys. Acta* **673**, 26-36.

Saitou, M., Fujimoto, K., Doi, Y., Itoh, M., Fujimoto, T., Furuse, M., Takano, H., Noda, T. and Tsukita, S. (1998). Occludin-deficient embryonic stem cells can differentiate into polarized epithelial cells bearing tight junctions. *J. Cell Biol.* **141**, 397-408.

Saitou, M., Furuse, M., Sasaki, H., Schulzke, J. D., Fromm, M., Takano, H., Noda, T. and Tsukita, S. (2000). Complex phenotype of mice lacking occludin, a component of tight junction strands. *Mol. Biol. Cell* **11**, 4131-4142.

Schultz, S. G. and Zalusky, R. (1964). Ion transport in isolated rabbit ileum. I. Short-circuit current and Na fluxes. *J. Gen. Physiol.* **47**, 567-584.

Simon, D. B., Lu, Y., Choate, K. A., Velazquez, H., Al-Sabban, E., Praga, M., Casari, G., Bettinelli, A., Colussi, G., Rodriguez-Soriano, J. et al. (1999). Paracellin-1, a renal tight junction protein required for paracellular Mg^{2+} resorption. *Science* **285**, 103-106.

Sonoda, N., Furuse, M., Sasaki, H., Yonemura, S., Katahira, J., Horiguchi, Y. and Tsukita, S. (1999). Clostridium perfringens enterotoxin fragment removes specific claudins from tight junction strands: Evidence for direct involvement of claudins in tight junction barrier. *J. Cell Biol.* **147**, 195-204.

Tsukita, S. and Furuse, M. (1998). Overcoming barriers in the study of tight junction functions: from occludin to claudin. *Genes Cells* **3**, 569-573.

Tsukita, S., Furuse, M. and Itoh, M. (2001). Multifunctional strands in tight junctions. *Nat. Rev. Mol. Cell. Biol.* **2**, 285-293.

Van Itallie, C., Rahner, C. and Anderson, J. M. (2001). Regulated expression of claudin-4 decreases paracellular conductance through a selective decrease in sodium permeability. *J. Clin. Invest.* **107**, 1319-1327.

Weiske, J., Schöneberg, T., Schröder, W., Hatzfeld, M., Tauber, R. and Huber, O. (2001). The fate of desmosomal proteins in apoptotic cells. *J. Biol. Chem.* **276**, 41175-41181.

Wilcox, E. R., Burton, Q. L., Naz, S., Riazuddin, S., Smith, T. N., Ploplis, B., Belyantseva, I., Ben-Yosef, T., Liburd, N. A., Morell, R. J. et al. (2001). Mutations in the gene encoding tight junction claudin-14 cause autosomal recessive deafness DFNB29. *Cell* **104**, 165-172.